

# The kinetic spherical model in a magnetic field

Matthias Paessens<sup>a,b</sup> and Malte Henkel<sup>a</sup>

<sup>a</sup>Laboratoire de Physique des Matériaux,<sup>1</sup> Université Henri Poincaré Nancy I,  
B.P. 239, F – 54506 Vandœuvre lès Nancy Cedex, France

<sup>b</sup>Institut für Festkörperforschung (Theorie II), Forschungszentrum Jülich, D – 52425 Jülich, Germany

## Abstract

The long-time kinetics of the spherical model in an external magnetic field and below the equilibrium critical temperature is studied. The solution of the associated stochastic Langevin equation is reduced exactly to a single non-linear Volterra equation. For a sufficiently small external field, the kinetics of the magnetization-reversal transition from the metastable to the ground state is compared to the ageing behaviour of coarsening systems quenched into the low-temperature phase. For an oscillating magnetic field and below the critical temperature, we find evidence for the absence of the frequency-dependent dynamic phase transition, which was observed previously to occur in Ising-like systems.

PACS numbers: 05.20.-y, 05.10.Gg, 75.10.Hk, 75.60.Ej, 02.30.Rz

---

<sup>1</sup>Laboratoire associé au CNRS UMR 7556

# 1 Introduction

Non-equilibrium critical phenomena are a subject of intense research activity. A common way to reach such a situation is through a rapid change of one of the macroscopic variables which enter into the equation of state. For definiteness, consider a simple ferromagnet. It may be brought out of equilibrium, for example, by starting initially from a fully disordered state and then quench the system rapidly to a temperature below the system's critical temperature  $T_c > 0$ . The resulting ageing behaviour has been in the focus of intensive study, see [1, 2, 3, 4, 5] for reviews. Another way to reach a non-equilibrium state is to start from a magnetically ordered state below  $T_c$  and then turn on a magnetic field  $H$  oriented antiparallel with respect to the magnetic order parameter. Then the system will find itself in a metastable stable and a magnetization reversal transition towards the stable ground state will take place, see [6, 7] for reviews.

After a quench to below  $T_c$ , the system undergoes phase-ordering, that is domains of a time-dependent typical size  $L(t) \sim t^{1/z}$  form and grow, where  $z$  is the dynamical exponent. As a consequence, a system of infinite size slowly evolves towards an equilibrium state, without ever reaching it. This evolution is more fully revealed through the study of *two-time* quantities, such as the two-time autocorrelation function  $C(t, s)$  and the autoresponse function  $R(t, s)$

$$C(t, s) = \langle \phi(t) \phi(s) \rangle , \quad R(t, s) = \left. \frac{\delta \langle \phi(t) \rangle}{\delta h(s)} \right|_{h=0} \quad (1.1)$$

where  $\phi$  is the order parameter,  $h$  the conjugate magnetic field,  $t$  is called the observation time and  $s$  the waiting time. Ageing occurs in the regime when  $s$  and  $\tau = t - s > 0$  are simultaneously much larger than any microscopic time scale  $\tau_{\text{micro}}$ . In many systems, one finds in the ageing regime a scaling behaviour, see [3, 4]

$$C(t, s) = s^{-b} f_C(t/s) , \quad R(t, s) = s^{-1-a} f_R(t/s) \quad (1.2)$$

where  $a$  and  $b$  are non-equilibrium exponents. For  $T < T_c$ ,  $b = 0$  while  $a$  depends on whether there are short-ranged or long-ranged correlations in the equilibrium state. For short-ranged correlations,  $a = 1/z$ , whereas for long-ranged correlations  $a = (d - 2 + \eta)/z$  [8]. The scaling functions behave for large arguments  $x = t/s \gg 1$  asymptotically as

$$f_C(x) \sim x^{-\lambda_C/z} , \quad f_R(x) \sim x^{-\lambda_R/z} \quad (1.3)$$

where  $\lambda_C$  and  $\lambda_R$  are the autocorrelation [9, 10] and autoresponse [11] exponents, respectively. While for a fully disordered initial state, it is traditionally accepted that  $\lambda_C = \lambda_R$ , for spatially long-ranged initial correlations of the form  $C_{\text{ini}}(\mathbf{r}) \sim |\mathbf{r}|^{-d-\alpha}$  (with  $\alpha \leq 0$ ) the relation  $\lambda_C = \lambda_R + \alpha$  has been conjectured [11]. Furthermore, the rigorous arguments of [12] readily yield  $\lambda_C \geq (d + \alpha)/2$ . Very recently, different exponents  $\lambda_C \neq \lambda_R$  have also been found in the random sine-Gordon model and in addition  $\lambda_C < d/2$  violates the rigorous bound mentioned above [13]. In addition, and going beyond these traditional scaling arguments, it has been proposed recently that the dynamical symmetry group of ageing systems might include more general transformations than merely the simple dynamical scaling as expressed by eq. (1.2). In particular, there is evidence that the dynamical group of ageing systems includes so-called local scale transformations related to conformal transformations in time [15]. If that is the case, the form of the scaling function

$$f_R(x) = r_0 x^{1+a-\lambda_R/z} (x - 1)^{-1-a} \quad (1.4)$$

is completely fixed ( $r_0$  is a normalization constant) [14, 15]. Going beyond phenomenological tests, at least for the case  $z = 2$  it can be shown that, given only the covariance of the response functions under

scale and also Galilei transformations, then a Ward identity guarantees the covariance under the full group of local scale transformations [16]. Furthermore, the causality condition  $R(t, s) = 0$  for  $t < s$  also follows in a model-independent way [16]. Tests of Galilei invariance require the consideration of space-time-dependent response functions, going beyond the autoresponse function  $R(t, s)$  of eq. (1.2). Indeed, the phase-ordering kinetics of the Glauber-Ising model has recently been shown to be Galilei-invariant in the ageing regime [17].

Another central question in this context is how to characterize whether/when under the conditions just described the system is in thermodynamic equilibrium. It is convenient to consider the fluctuation-dissipation ratio [18, 19]

$$X(t, s) = TR(t, s) \left( \frac{\partial C(t, s)}{\partial s} \right)^{-1} \quad (1.5)$$

At equilibrium, the fluctuation-dissipation theorem states that  $X(t, s) = 1$ . The breaking of the fluctuation-dissipation theorem has been investigated intensively both theoretically (see e.g. [3, 4, 20, 21, 5]) and experimentally [22, 23, 24].

Here we are interested in the non-equilibrium behaviour associated with the magnetization-reversal transition from the metastable to the equilibrium state. This problem has also received intense attention, both experimentally (e.g. [25, 26, 27]) and theoretically, see [28, 29, 30, 31, 32, 33, 34]. What can be learned from the study of two-time quantities about this process? Additional insight may be obtained by studying the system's response to a time-dependent, e.g. oscillating, magnetic field and we shall study whether there exists a dynamic phase-transition at a finite and non-vanishing value of the period  $P$  of the field [35, 36]. Surprisingly, there is *no* such transition in the spherical model, although it is known to occur e.g. in the 2D Ising model.

In order to obtain explicit analytical results, we shall study the effects of a magnetic field in the kinetic mean spherical model, to be defined precisely in section 2. This is one of the very few models which can be solved exactly in a great variety of circumstances and has been studied in detail in the past, either in the context of continuum field theories [37, 38, 39, 40, 41, 42, 43] or else in the form of a lattice model [44, 45, 46, 47, 48, 49, 11, 50]. It is known that in  $d < 4$  dimensions, the spherical model yields results distinct from mean-field theory and therefore permits the study of fluctuation effects. In addition, we recall that experimental results of the magnetization reversal [25, 26] are usually described in terms of an anisotropic Heisenberg model. Recall that the spherical model shares the following *equilibrium* properties with the O(3) Heisenberg model and which distinguish it from the often-used Ising model:

- it has a continuous symmetry ( $O(n)$  in the  $n \rightarrow \infty$  limit).
- there is no equilibrium phase-transition in 2D.
- the equilibrium specific heat exponent  $\alpha < 0$  in 3D.

These similarities might suggest that qualitatively the kinetics of spherical and the O(3) Heisenberg models should be closer to each other than either is to the kinetics of the Ising model. Still, the spherical model should be considered a toy model certainly not meant to be physically realistic.

This paper is organized as follows. In section 2, the model is defined and the exact solution outlined. All physical quantities can be expressed in terms of the time-dependent solution  $g(t)$  of a nonlinear Volterra integral equation. In section 3, the solution of this equation and its asymptotics are discussed. In sections 4 and 5, single- and two-time observables are calculated for the full time-range of the magnetization-reversal transition for constant magnetic fields and in section 6 time-dependent fields

are considered. Section 7 presents our conclusions. In the appendices, we comment on the numerical techniques and study the exact long-time behaviour of the Volterra equation.

## 2 Model and formalism

We begin by recalling the definition of the kinetic mean spherical model, using the formalism as exposed in [44, 45, 47, 11]. We consider a system of time-dependent classical spin variables  $S_{\mathbf{x}}(t)$  located on the sites  $\mathbf{x}$  of a  $d$ -dimensional hypercubic lattice. They may take arbitrary real values subject only to the mean spherical constraint

$$\sum_{\mathbf{x}} \langle S_{\mathbf{x}}(t)^2 \rangle = \mathcal{N} \quad (2.1)$$

where  $\mathcal{N}$  is the number of sites of the lattice. The role of imposing the spherical constraint either microscopically or rather in the mean (which is the only case where the dynamics can be solved) has been carefully studied recently [43]. Provided the infinite-volume limit is taken *before* the long-time limit, either way of treating the spherical constraint leads to the same results.

The spherical model Hamiltonian reads

$$\mathcal{H} = -J \sum_{\langle \mathbf{x}, \mathbf{y} \rangle} S_{\mathbf{x}}(t) S_{\mathbf{y}}(t) - \sum_{\mathbf{x}} H_{\mathbf{x}}(t) S_{\mathbf{x}}(t) \quad (2.2)$$

where  $H_{\mathbf{x}}(t)$  is the space- and time-dependent external magnetic field. The first sum extends over nearest-neighbour pairs only and the second sum over the entire lattice. We choose units such that  $J = 1$ . The system is supposed to be translation-invariant in all directions. The kinetics is assumed to be described in terms of a Langevin equation

$$\frac{dS_{\mathbf{x}}(t)}{dt} = \sum_{\mathbf{y}(\mathbf{x})} S_{\mathbf{y}}(t) - (2d + \mathfrak{z}(t)) S_{\mathbf{x}}(t) + H_{\mathbf{x}}(t) + \eta_{\mathbf{x}}(t) \quad (2.3)$$

where the sum over  $\mathbf{y}$  extends over the nearest neighbours of  $\mathbf{x}$ . The gaussian noise  $\eta_{\mathbf{x}}(t)$  describes that the model is in contact with a heat bath. It is characterized by a vanishing ensemble-average and the second moment

$$\langle \eta_{\mathbf{x}}(t) \eta_{\mathbf{y}}(t') \rangle = 2T \delta_{\mathbf{x}, \mathbf{y}} \delta(t - t') \quad (2.4)$$

Finally, the function  $\mathfrak{z}(t)$  is fixed by the mean spherical constraint (2.1) and has to be determined.

By a Fourier transformation

$$\tilde{f}(\mathbf{q}) = \sum_{\mathbf{r}} f_{\mathbf{r}} e^{-i\mathbf{q} \cdot \mathbf{r}} , \quad f_{\mathbf{r}} = (2\pi)^{-d} \int_{\mathcal{B}} d\mathbf{q} \tilde{f}(\mathbf{q}) e^{i\mathbf{q} \cdot \mathbf{r}} \quad (2.5)$$

where the integral is taken over the first Brillouin zone  $\mathcal{B}$ , the Fourier-transformed spin variable  $\tilde{S}(\mathbf{q}, t)$  becomes

$$\tilde{S}(\mathbf{q}, t) = \frac{e^{-\omega(\mathbf{q})t}}{\sqrt{g(t)}} \left[ \tilde{S}(\mathbf{q}, 0) + \int_0^t dt' e^{\omega(\mathbf{q})t'} \sqrt{g(t')} \left[ \tilde{H}(\mathbf{q}, t') + \tilde{\eta}(\mathbf{q}, t') \right] \right] \quad (2.6)$$

with the dispersion relation

$$\omega(\mathbf{q}) = 2 \sum_{i=1}^d (1 - \cos(q_i)) \quad (2.7)$$

and we have also defined

$$g(t) = \exp \left( 2 \int_0^t dt' \mathfrak{z}(t') \right) \quad (2.8)$$

Clearly, the time-dependence of  $\tilde{S}(\mathbf{q}, t)$  and any correlators will be given in terms of the function  $g = g(t)$ .

We now derive the expressions for the correlators and response functions for an arbitrary external field  $H_{\mathbf{x}}(t)$  and general initial conditions. Consider the two-time spin-spin correlation function

$$C_{\mathbf{x},\mathbf{y}}(t, s) = C_{\mathbf{x}-\mathbf{y}}(t, s) = \langle S_{\mathbf{x}}(t) S_{\mathbf{y}}(s) \rangle = (2\pi)^{-2d} \int_{\mathcal{B}^2} d\mathbf{q} d\mathbf{q}' e^{i(\mathbf{q} \cdot \mathbf{x} + \mathbf{q}' \cdot \mathbf{y})} \langle \tilde{S}(\mathbf{q}, t) \tilde{S}(\mathbf{q}', s) \rangle \quad (2.9)$$

A straightforward calculation gives

$$\begin{aligned} \tilde{C}(\mathbf{q}, \mathbf{q}'; t, s) &= \langle \tilde{S}(\mathbf{q}, t) \tilde{S}(\mathbf{q}', s) \rangle \\ &= \frac{e^{-\omega(\mathbf{q})t - \omega(\mathbf{q}')s}}{\sqrt{g(t)g(s)}} \left[ (2\pi)^d \delta^d(\mathbf{q} + \mathbf{q}') \left( \tilde{C}(\mathbf{q}, t) + 2T \int_0^t dt' e^{2\omega(\mathbf{q})t'} g(t') \right) \right. \\ &\quad + \langle \tilde{S}(\mathbf{q}', 0) \rangle \int_0^t dt' e^{\omega(\mathbf{q})t'} \sqrt{g(t')} \tilde{H}(\mathbf{q}, t') + \langle \tilde{S}(\mathbf{q}, 0) \rangle \int_0^s ds' e^{\omega(\mathbf{q}')s'} \sqrt{g(s')} \tilde{H}(\mathbf{q}', s') \\ &\quad \left. + \int_0^t dt' e^{\omega(\mathbf{q})t'} \sqrt{g(t')} \tilde{H}(\mathbf{q}, t') \int_0^s ds' e^{\omega(\mathbf{q}')s'} \sqrt{g(s')} \tilde{H}(\mathbf{q}', s') \right] \end{aligned} \quad (2.10)$$

where  $\tilde{C}(\mathbf{q}, t)$  is the single-time correlator. Here the average was carried out over the noise and the initial conditions  $S_{\mathbf{x}}(0)$  such that

$$\langle \tilde{S}(\mathbf{q}, 0) \rangle = \sum_{\mathbf{x}} \langle S_{\mathbf{x}}(0) \rangle e^{-i\mathbf{q} \cdot \mathbf{x}} = (2\pi)^d \delta^d(\mathbf{q}) S_0 \quad (2.11)$$

In direct space, the two-time autocorrelator becomes

$$\begin{aligned} C_{\mathbf{x},\mathbf{x}}(t, s) &= (2\pi)^{-2d} \int_{\mathcal{B}^2} d\mathbf{q} d\mathbf{q}' e^{i(\mathbf{q} + \mathbf{q}') \cdot \mathbf{x}} \tilde{C}(\mathbf{q}, \mathbf{q}'; t, s) \\ &= \frac{1}{\sqrt{g(t)g(s)}} \left[ A\left(\frac{t+s}{2}\right) + 2T \int_0^s du f\left(\frac{t+s}{2} - u\right) g(u) \right. \\ &\quad + S_0 \int_0^t dt' B_{\mathbf{x}}(t') \sqrt{g(t')} + S_0 \int_0^s ds' B_{\mathbf{x}}(s') \sqrt{g(s')} \\ &\quad \left. + \int_0^t dt' B_{\mathbf{x}}(t') \sqrt{g(t')} \int_0^s ds' B_{\mathbf{x}}(s') \sqrt{g(s')} \right] \end{aligned} \quad (2.12)$$

where we have defined

$$\begin{aligned} f(t) &= (2\pi)^{-d} \int_{\mathcal{B}} d\mathbf{q} e^{-2\omega(\mathbf{q})t} = (e^{-4t} I_0(4t))^d \\ A(t) &= (2\pi)^{-d} \int_{\mathcal{B}} d\mathbf{q} e^{-2\omega(\mathbf{q})t} \tilde{C}(\mathbf{q}, 0) \\ B_{\mathbf{x}}(t) &= (2\pi)^{-d} \int_{\mathcal{B}} d\mathbf{q} e^{\omega(\mathbf{q})t + i\mathbf{q} \cdot \mathbf{x}} \tilde{H}(\mathbf{q}, t) \end{aligned} \quad (2.13)$$

and  $I_0$  is a modified Bessel function [51]. We see explicitly how the initial magnetization  $S_0$  and the initial correlator  $C_{\mathbf{x}}(0)$  affect the dynamics of the system.

It remains to determine the function  $g(t)$ . Because of the spherical constraint (2.2) and spatial translation invariance, the equal-time autocorrelator must satisfy

$$C_0(t, t) = \int_{\mathcal{B}} d\mathbf{q} \tilde{C}(\mathbf{q}, t) = \langle S_{\mathbf{x}}(t)^2 \rangle = 1 \quad (2.14)$$

This in turn fixes  $\mathfrak{z}(t)$  or via (2.8) the function  $g(t)$  as the solution of a nonlinear Volterra integral equation

$$g(t) = A(t) + 2T \int_0^t dt' f(t-t')g(t') + 2S_0 \int_0^t dt' B_{\mathbf{x}}(t') \sqrt{g(t')} + \left( \int_0^t dt' B_{\mathbf{x}}(t') \sqrt{g(t')} \right)^2 \quad (2.15)$$

For  $S_0 = 0$  and  $T = 0$ , eqs. (2.12,2.15) had been derived before for the spherical spin-glass [45]. Besides on time,  $g(t)$  also depends on the temperature  $T$  and the initial conditions parametrized by  $S_0$  and  $C_{\mathbf{x}}(0)$ .

The expressions for  $A(t)$  and  $B_{\mathbf{x}}(t)$  simplify in certain cases. For uncorrelated initial conditions

$$C_{\mathbf{x},\mathbf{y}}(0) = (1 - S_0^2) \delta_{\mathbf{x},\mathbf{y}} + S_0^2 \quad (2.16)$$

Then  $\tilde{C}(\mathbf{q}, 0) = 1 - S_0^2 + (2\pi)^d \delta^d(\mathbf{q}) S_0^2$  and

$$A(t) = (1 - S_0^2) f(t) + S_0^2 \quad (2.17)$$

For a spatially uniform magnetic field  $H_{\mathbf{x}}(t) = H(t)$  we have

$$B_{\mathbf{x}}(t) = H(t) \quad (2.18)$$

These two conditions and consequently eqs. (2.17,2.18) will be used throughout this paper.

When  $S_0 \neq 0$ , it will be useful to consider besides  $C(t, s)$  also the connected two-time autocorrelator (see [11] for an analogous situation in the 1D Glauber-Ising model)

$$\Gamma(t, s) = \langle S_{\mathbf{x}}(t) S_{\mathbf{x}}(s) \rangle - \langle S_{\mathbf{x}}(t) \rangle \langle S_{\mathbf{x}}(s) \rangle \quad (2.19)$$

Finally, the response function is obtained in the usual way [39, 40, 44, 45, 47, 11] by considering the linear response to the magnetic field. It is easy to see that in Fourier space

$$\tilde{R}(\mathbf{q}, t, s) = \frac{\delta \langle \tilde{S}(\mathbf{q}, t) \rangle}{\delta \tilde{h}(\mathbf{q}, s)} \bigg|_{h_r=0} = e^{-\omega(\mathbf{q})(t-s)} \sqrt{\frac{g(s)}{g(t)}} \quad (2.20)$$

From these expressions, the autocorrelation function  $C(t, s) = C_0(t, s)$  and the autoresponse function  $R(t, s) = R_0(t, s)$  can be obtained by integrating over the momentum  $\mathbf{q}$ .

Summarizing, the physically interesting correlation and response functions are given by equations (2.12,2.19,2.20) together with the constraint eq. (2.15). This constitutes the main result of the general formalism.

In the next section, we turn towards the solution of these equations. Compared to the case without an external magnetic field, this task is difficult since the underlying Volterra equation (2.15) is nonlinear. The mathematical theory of nonlinear Volterra equations is still being developed [52]. In a few cases, explicit analytic solutions can be found. Otherwise, we shall turn to numerical methods.

### 3 Solution of the constraint

It is the peculiar feature of the kinetic spherical model that a complicated many-body problem can be exactly reduced to the solution of a single equation. We first derive the exact late-time asymptotic behaviour of the solution  $g(t)$  of eq. (2.15) for a constant field  $H(t) = H$ , that is for times  $t \gg 1$ . Afterwards, we comment on the use of asymptotic expansions for the calculation of physical observables.

It is convenient to consider first the initial condition  $S_0 = 0$  which is easier to handle. As we shall see, the system actually loses its memory of the initial state quite rapidly.

A first condition on the late-time asymptotics comes from the known fact  $|C_{\mathbf{x},\mathbf{x}}| \leq 1$ . Together with eq. (2.12), it is easy to see that the power-law dependence of  $g(t)$  on  $t$  as found [47] for the special case  $H = 0$  and  $T < T_c$  is incompatible with that condition in the case at hand.

We therefore try, for late times  $t \gg 1$ , an asymptotic exponential ansatz

$$g(t) = a e^{t/\tau}, \quad (3.1)$$

where  $a$  and  $\tau$  are constants to be determined. Indeed eq. (2.12) now shows that  $|C_{\mathbf{x},\mathbf{x}}|$  is bounded if  $\tau > 0$ . To see this, observe that because of the ansatz (3.1) the main contribution to the terms in eq. (2.12) which depend on the magnetic field comes from the upper limit of integration. Consequently, the quadratic term in  $B_{\mathbf{x}}(t)$  dominates over the terms linear in  $B_{\mathbf{x}}(t)$  and also over those terms which do not contain  $B_{\mathbf{x}}(t)$  at all. For large times  $t, s$  we have asymptotically

$$\lim_{t,s \rightarrow \infty} C_{\mathbf{x},\mathbf{x}}(t, s) = 4H^2\tau^2, \quad (3.2)$$

where the limit is taken for a constant time difference  $\sigma = t - s \geq 0$ . Inserting eq. (3.1) into eq. (2.15) yields for  $S_0 = 0$ , along the same lines

$$g(t) = A(t) + 2T \int_0^t dt' f(t - t') g(t') + 4H^2\tau^2 g(t). \quad (3.3)$$

and with  $f(t) = (e^{-4t} I_0(4t))^d$  from eq. (2.13). Using the Laplace transformation

$$\bar{f}(p) = \int_0^\infty dt f(t) e^{-pt} \quad (3.4)$$

we find from (3.3)

$$\bar{g}(p) = \frac{\bar{A}(p)}{1 - 2T\bar{f}(p) - 4H^2\tau^2} \quad (3.5)$$

This must be consistent with the Laplace-transformed ansatz of eq. (3.1)

$$\bar{g}(p) = \frac{a}{p - \tau^{-1}}. \quad (3.6)$$

These two expressions can only be compatible if the denominator in eq. (3.5) vanishes at  $p = \tau^{-1}$ , i.e.

$$1 - 2T\bar{f}(\tau^{-1}) = 4H^2\tau^2 \quad (3.7)$$

and this must be a simple intersection (from eq. (2.17) we know that  $A(t) > 0$ , therefore  $\bar{A}(p) > 0$  can be related to  $a$ ). Eq. (3.7) is an implicit equation for  $\tau$  and we now show that there is always an unique solution, provided  $H \neq 0$ .

First, we consider the case  $\tau \rightarrow 0$ . From the definition of  $\bar{f}(p)$  and  $f(t) > 0$ , we have  $\bar{f}(p) > 0$ . Similarly,  $f(t) \leq 1$  for  $t \geq 0$  implies  $\bar{f}(p) \leq p^{-1}$ . Therefore

$$\lim_{\tau \rightarrow 0} (1 - 2T\bar{f}(\tau^{-1})) = 1 \quad (3.8)$$

Second, we consider the case  $\tau \rightarrow \infty$ . From the results of [47] on  $\bar{f}(p)$  one has

$$\lim_{\tau \rightarrow \infty} (1 - 2T\bar{f}(\tau^{-1})) = 1 - \frac{T}{T_c} \quad (3.9)$$

It is well-known that the Laplace transformation  $\bar{f}(p)$  of a positive function  $f(t)$  decreases monotonously with  $p$  [51]. Therefore, the left-hand-side of eq. (3.7) decreases monotonously from 1 to  $1 - T/T_c$  as  $\tau$  increases from 0 to  $\infty$ , while the right-hand-side  $\sim \tau^2$  increases monotonously for  $H \neq 0$ . This establishes the existence of a simple intersection and therefore of a unique  $\tau$  which describes the late-time asymptotics of  $g(t)$  for  $H \neq 0$ , see eq. (3.1). For  $|H| \rightarrow 0$  and  $T \leq T_c$  we find  $\tau \rightarrow \infty$ , while for  $H = 0$  a solution for  $\tau$  only exists if  $T > T_c$ . This reproduces the well-known result that for  $H = 0$ ,  $g(t)$  only has an exponential behaviour for  $T > T_c$  [47, 11]. The fact that in the case  $H \neq 0$  we find an exponential behaviour for all temperatures  $T$  shows that the system relaxes to an equilibrium state after the finite time  $\tau$  [45] and neither critical behaviour nor ageing is expected for late times. It is now clear that adding the extra terms coming in for  $S_0 \neq 0$  will merely generate sub-leading corrections and the asymptotic solution eq. (3.1) will not be affected.

In conclusion, we have established: *the leading long-time asymptotic behaviour of  $g(t)$  is given by eq. (3.1) where  $\tau$  is the unique solution of eq. (3.7) and with  $a = -\bar{A}(1/\tau)/(2T\bar{f}'(1/\tau))$ , for any value  $H \neq 0$  of the constant magnetic field and any given mean initial magnetization  $S_0$ .*

For finite times, there is no analytical solution of eq. (2.15) available. Instead, as described in appendix A, we determine  $g(t)$  numerically. Although the two-time observables are the relevant quantities for the study of ageing phenomena (see section 4), it is still useful to consider single-time observables like the average magnetization  $S(t)$  given by

$$S(t) = \langle S_{\mathbf{x}}(t) \rangle = \frac{1}{\sqrt{g(t)}} \left[ S_0 + \int_0^t dt' H(t') \sqrt{g(t')} \right] \quad (3.10)$$

In practise, care is required in using asymptotic solutions of  $g(t)$  for the prediction of the time-dependence of observables such as  $S(t)$ . We illustrate this in figure 1, where  $g(t)$  and the distance of the magnetization to its equilibrium value  $S_{\infty} - S(t)$  are shown as a function of time. We see in figure 1a that after an initial fall-off,  $g(t)$  quickly reaches the asymptotical regime of exponential growth. In figure 1b, however, we compare the mean magnetization  $S(t)$  as found from the exact numerical solution  $g(t)$  (see appendix A) with the one obtained from an asymptotic fit of the form

$$g(t) \simeq e^{t/\tau} \sum_{\ell=0}^{\ell_{\max}} a_{\ell} (t - t_0)^{-\ell} \quad (3.11)$$

where we use  $\ell_{\max} = 5$ . Although that asymptotic fit for  $g(t)$  cannot be distinguished from the exact numerical result in figure 1a, the deviation in  $S(t)$  is considerable.

In the rest of this paper, we shall use the direct numerical solution of eq. (2.15).

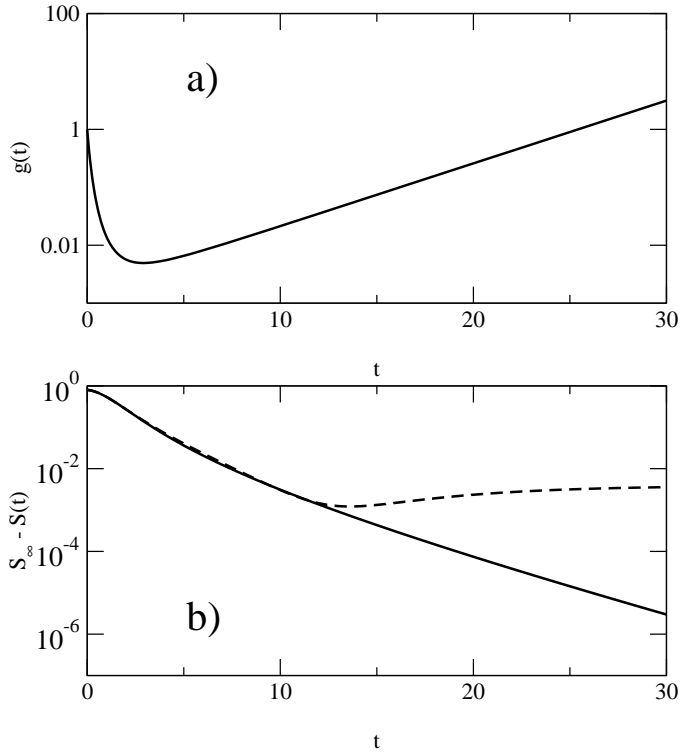


Figure 1: The function  $g(t)$  (a) and the distance of the magnetization to its equilibrium value (b) for  $d = 3.5$ ,  $T = 2$  ( $T_c \approx 5.27$ ),  $H = 0.1$  and  $S_0 = 0$ . The full curve shows the results for the direct numerical calculation, the dashed line shows the results for the 5th order fit which coincides with the full curve in (a).

## 4 Single-time observables

Our first applications consider single-time observables, which are the ones most commonly studied.

An instructive example on the importance of fluctuation effects is constructed as follows. For a given external magnetic field  $H$ , one may easily calculate the equilibrium magnetization  $M_{\text{eq}}$ . Now prepare the system such that the spins have a mean magnetization  $M_{\text{eq}}$  but such that spins on different sites are uncorrelated. The time evolution of  $S(t)$  is shown in figure 2. While a mean-field description would have predicted a constant  $S(t)$ , we see that the magnetization is not constant but increases towards a peak before it falls back to the equilibrium value  $M_{\text{eq}}$ . Intuitively, we would expect that the individual spins tend to align with the local magnetic field provided by their neighbours. Since initially  $S_0 = M_{\text{eq}} > 0$ , one orientation is preferred with respect to the other one and domains oriented in parallel to  $M_{\text{eq}}$  will grow preferentially. When the domains have grown large enough the influence of this effect decreases and the system approaches quickly the equilibrium and the magnetization decreases again. This picture, although close in spirit to the Ising model with its discrete spin variables, also works in the spherical model, in spite of the fact that the interaction can be reduced to a free-field theory. The remnant interaction between different spins provided by the spherical constraint is sufficient to achieve non-trivial correlations between different spins.

We have seen in the previous section that for  $H \neq 0$  and very late times the system relaxes back to its unique equilibrium state. For a vanishing magnetic field, the equilibrium free energy would have a double-well structure with two equivalent minima, corresponding to the two possible orientations of the mean magnetization. Turning on a magnetic field, this potential is tilted and the depth of the two local

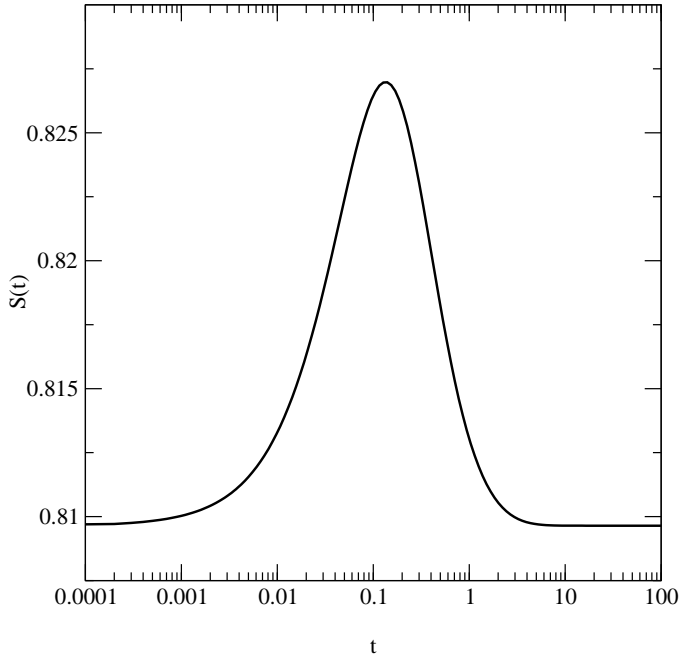


Figure 2: The magnetization of the system evolving from  $S_0 = S_\infty$  calculated for  $d = 3.5$ ,  $T = 2$  ( $< T_c$ ),  $H = 0.2$  and  $S_0 \approx 0.810$ .

minima is no longer the same. The lower minimum becomes the unique equilibrium state, the other one corresponds to a metastable state. It is clear that if the system is initially prepared in the well corresponding to the equilibrium state, it will relax rapidly towards that state. Here we are interested how the transition from the metastable state towards the equilibrium state occurs.

Therefore, we prepare the system with an initial magnetization antiparallel to the given external field. In figure 3a we show the time evolution of the mean magnetization. After a short time the system reaches the metastable state, independently of the absolute value of the initial magnetization  $S_0$ , and where  $S(t)$  stays practically constant. The system remains in the metastable state for several decades until the magnetization is reversed quite rapidly (although one should not be misled by the logarithmic time-scale in this figure which makes the changeover to appear be very fast). In order to understand better what is going on we define a characteristic length  $\lambda(t)$  of the *fluctuations*

$$\lambda(t)^2 = \sum_{\mathbf{r} \in \Lambda} \mathbf{r}^2 (C_{\mathbf{r}}(t, t) - S(t)^2), \quad (4.1)$$

where  $\mathbf{r}$  runs over all sites of the lattice  $\Lambda \subset \mathbb{Z}^d$  and  $C_{\mathbf{r}}(t, s)$  is the spin–spin correlation function (2.9). The time evolution of  $\lambda(t)$  is shown in figure 3b. Starting from a very small initial value,  $\lambda(t)$  increases towards a maximum value which is reached at the time when  $S(t)$  starts to deviate perceptively from its value in the metastable state. While  $S(t)$  changes its sign,  $\lambda(t)$  remains approximately constant at its maximal values before it relaxes towards the equilibrium correlation length, with a typical value of a few lattice spacings. The coincidence of the times of the reversal of  $S(t)$  and the peak in  $\lambda(t)$  shows that whole domains rather than single uncorrelated spins are flipping.

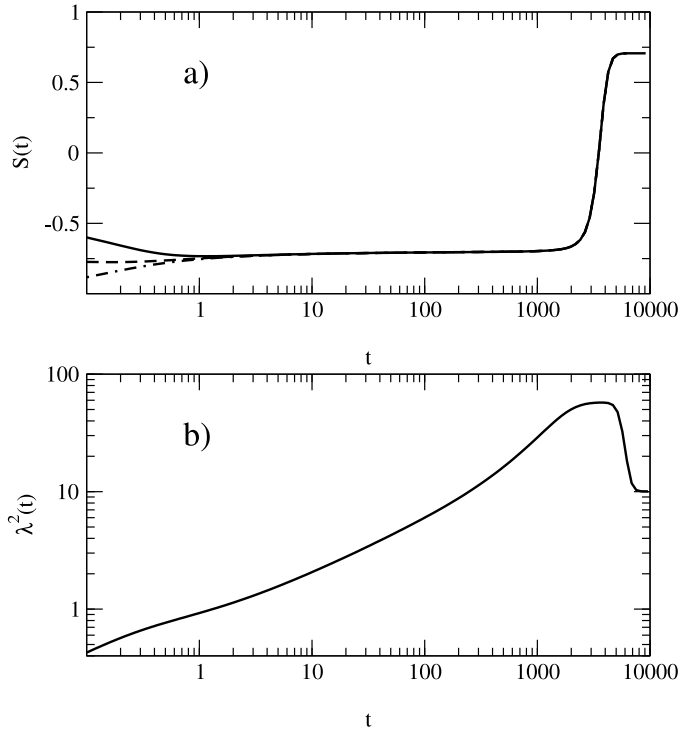


Figure 3: (a) Average magnetization  $S(t)$  for  $d = 3$ ,  $T = 2$  ( $< T_c \simeq 3.96$ ),  $H = 10^{-3}$  and  $S_0 = -0.5$  (full curve),  $S_0 = -0.75$  (dashed curve) and  $S_0 = -1$  (dash-dotted curve). (b) Squared correlation length  $\lambda(t)^2$  of fluctuations for  $S_0 = -0.5$ , where the other parameters are as in (a).

## 5 Two-time observables

Having seen that the magnetization reversal passes via an intermediate state with highly correlated fluctuations, we discuss in this section how this manifests itself in the behaviour of the two-time quantities. An important quantity is the time  $\vartheta$  after which the magnetization reverses itself. Evidently,  $\vartheta = \vartheta(H, T, d)$ , but we have not investigated in detail how  $\vartheta$  depends on these parameters in detail. For illustration purposes, we shall use in this section the same choice of parameter values as in figure 3, then  $\vartheta \approx 3000$ . For finite values of  $t$ ,  $g(t)$  can be readily found from eq. (2.15) using the numerical methods described in appendix A. We shall focus on the metastable state by restricting to waiting times  $s$  in the intermediate time regime  $s \leq \vartheta$ . A magnetization reversal is seen if the initial magnetization is chosen antiparallel to the external field.

Our choice of initially uncorrelated spin with a mean magnetization  $S_0$  can be considered as a special case of initially correlated spins. The case of spatial long-range correlations of the form  $C_{\text{ini}}(\mathbf{r}) \sim |\mathbf{r}|^{-d-\alpha}$  in the initial state was studied in detail before [39, 11]. Formally, this reduces to an initial state with a constant mean magnetization in the limit  $\alpha \rightarrow -d$ . Using the exact results of [11] for  $T < T_c$ , we have

$$\begin{aligned} C(t, s) &= 1 - \frac{T}{T_c} = M_{\text{eq}}^2 \\ R(t, s) &= [4\pi(t - s)]^{-d/2}, \end{aligned} \tag{5.1}$$

where  $M_{\text{eq}}$  is the equilibrium magnetization.

In figure 4a the correlation function  $C(t, s)$  is plotted versus the time difference  $t - s$  for several values of the waiting times  $s$  which are chosen to be in the metastable state, that is  $s \leq \vartheta$  (compare figure 3a). After a short time the curves reach a plateau, with a value very close to the equilibrium

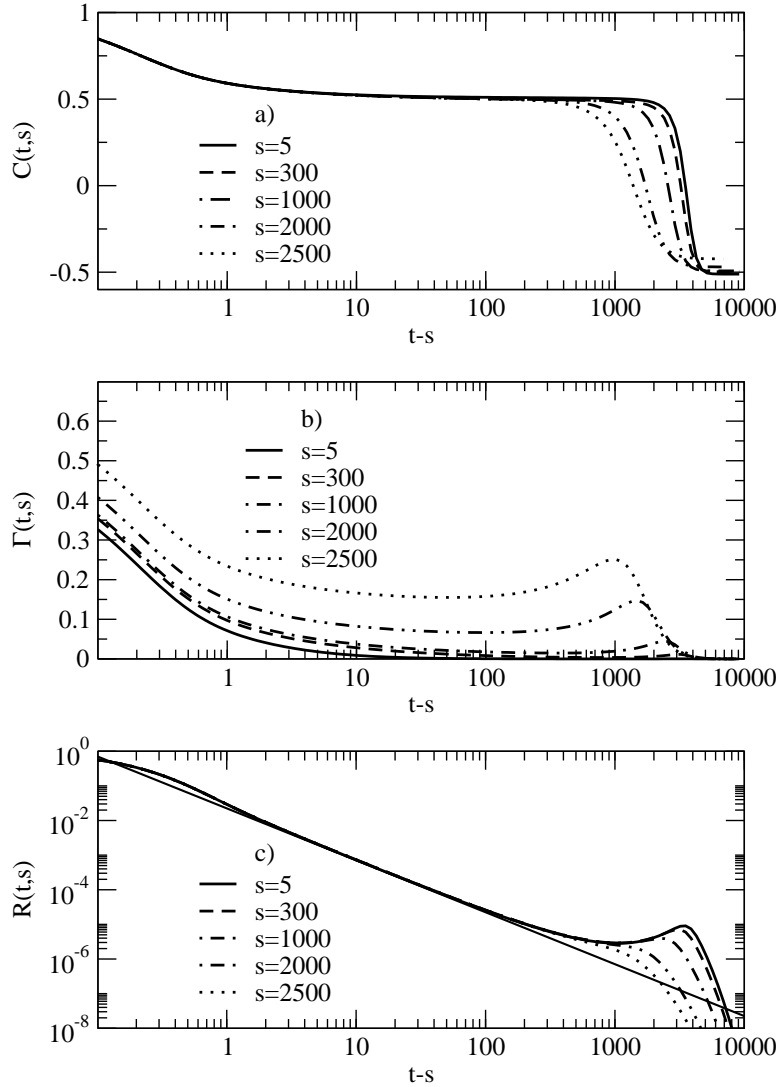


Figure 4: The two-time autocorrelation function  $C(t, s)$  (a), the correlation of fluctuations  $\Gamma(t, s)$  (b) and the response function  $R(t, s)$  (c) plotted vs. the time difference  $t - s$  for waiting times  $s = \{5; 300; 1000; 2000; 2500\}$ ; the data were calculated for  $d = 3$ ,  $T = 2$  and  $H = 10^{-3}$ . In (c) the straight line shows the formula  $[4\pi(t - s)]^{-d/2}$ .

value  $C(t, s) = M_{\text{eq}}^2$  (a small contribution of the magnetic field can be neglected here).  $C(t, s)$  maintains itself at this value for approximatively three decades, independently of the waiting time  $s$ . When the observation time  $t$  becomes larger than the magnetization reversal time  $\vartheta$ , the correlation function  $C(t, s)$  changes its sign because the spins at time  $s$  before the reversal are anticorrelated to the spins at time  $t$  after the reversal. However, we point out that the changeover takes more time when the waiting time  $s$  is increased. The curves rapidly approach the expected value  $-M_{\text{eq}}^2$  because spins of the metastable state are compared to the stable state. So we conclude that the correlation function  $C(t, s)$  is mainly determined by the value of magnetization.

While  $C(t, s)$  measures the time-dependence of the autocorrelation of a given spin,  $\Gamma(t, s)$ , see eq. (2.19), measures the fluctuations. This is shown in figure 4b. It can be seen that for waiting times  $s \leq 1000$ ,  $\Gamma(t, s)$  decreases fairly rapidly as a function of the time difference  $t - s$ . In addition, a small peak is observed in the region  $t \approx \vartheta$ . But for waiting times closer to the magnetization reversal time  $\vartheta$  (here for  $s = 2000$  and  $s = 2500$ ), the fluctuations have become quite substantial and show a larger peak

around  $(t - s) + s \approx \vartheta$ . This may be viewed as another hint for the existence of correlated domains: as the spins inside of a domain are highly correlated a fluctuation of a spin within such a domain will cause other spins in the domain to follow this fluctuation. In turn, a side-effect of the enhanced correlations is a longer lifetime of a spin fluctuation. After the magnetization reversal,  $\Gamma(t, s)$  rapidly falls to zero.

Finally, in figure 4c the response function  $R(t, s)$  is shown. First, we observe that for a time region of at least two decades we recover eq. (5.1), which was derived in [11] for the case without an external field. In this region translation invariance holds and hence no ageing occurs. The system behaves as if it were in equilibrium although it is only in a metastable state. Second, for observation times  $t$  getting closer to the reversal time  $\vartheta$ , the response function begins to deviate from this simple behaviour. We point out that the curves for all waiting times  $s$  still collapse onto each other and that this deviation occurs although  $C(t, s)$  still has not appreciably changed away from  $M_{\text{eq}}^2$ . Third, for times  $t \gtrsim \vartheta$  the dependence on the waiting times becomes obvious before the response curves decrease very fast. This can be explained by considering that the memory of perturbations is lost during the reversal from the metastable to the stable state.

In order to decide whether the system is in equilibrium or not we shall investigate now the zero-field-cooled (ZFC) magnetization which is defined by

$$M_{\text{ZFC}} = HT \int_s^t du R(t, u). \quad (5.2)$$

This quantity may be related to the fluctuation-dissipation ratio using eq. (1.5). Because of the non-vanishing initial magnetization  $S_0$  and the presence of an external magnetic field, the quantities  $C(t, s)$  and  $\Gamma(t, s)$  are different and a fluctuation-dissipation ratio is better defined using  $\Gamma(t, s)$ , namely  $X(t, s) = TR(t, s) (\partial\Gamma(t, s)/\partial s)^{-1}$ . This had been checked explicitly in the 1D Glauber-Ising model [11]. In spin glasses, it had been shown [18, 19] from mean-field theory that  $X = X(C(t, s))$  although that is not necessarily so beyond mean field or in simple ferromagnets [47, 53, 54]. Nevertheless, this assumption is of good heuristic value. In the spirit of the enterprise, let us consider the case where here  $X = X(\Gamma(t, s))$ . This amounts to saying that  $\Gamma$  serves as a clock for the evolution of the system. Then

$$M_{\text{ZFC}}/H = \int_{\Gamma(t, s)}^{\Gamma(t, t)} d\Gamma X(\Gamma). \quad (5.3)$$

Consequently, when plotting  $M_{\text{ZFC}}(t, s)/H$  versus  $\Gamma(t, s)$  for fixed  $s$  (see figure 5) the slope of the curve corresponds to the value of  $X$  – provided of course that the assumptions leading to (5.3) are valid.<sup>2</sup> Rather, we find in figure 5 that with increasing waiting time  $s$  the curves move from the lower right to the upper left. On the other hand, for a given value of  $s$ , the system starts in the lower right corner and moves rapidly along a curve  $M_{\text{ZFC}}(\Gamma) = \Gamma_0 - \Gamma$  until the metastable value  $M_{\text{ZFC}}/H = 1 - M_{\text{meta}} \simeq 1 - M_{\text{eq}}$  is reached. The slope of unity of this curve is the same as would be found for an equilibrium system. Surprisingly, while it undergoes the magnetization reversal, the system then passes through a loop, which corresponds to the peak in  $\Gamma(t, s)$ , before it reaches a horizontal line, of height  $1 - M_{\text{eq}}$ . The movement along the horizontal line is a behaviour typical of the low-temperature phase, indeed through the magnetization reversal the system behaves as if the quasiequilibrium branch close to the metastable state had to be joined with the low-temperature behaviour after the magnetization reversal. All in all, this behaviour is quite analogous to the one observed for  $M_{\text{ZFC}}$  as a function of  $C(t, s)$  for systems brought into the two-phase region by a temperature quench [56].

Of course, all the results in this section depend on having taken  $s \leq \vartheta$ . If we take instead  $s > \vartheta$ , the system quickly relaxes to its unique equilibrium state.

<sup>2</sup>For metastable systems with detailed balance and for time-scales shorter than the nucleation time, a fluctuation-dissipation relation is discussed in [55].

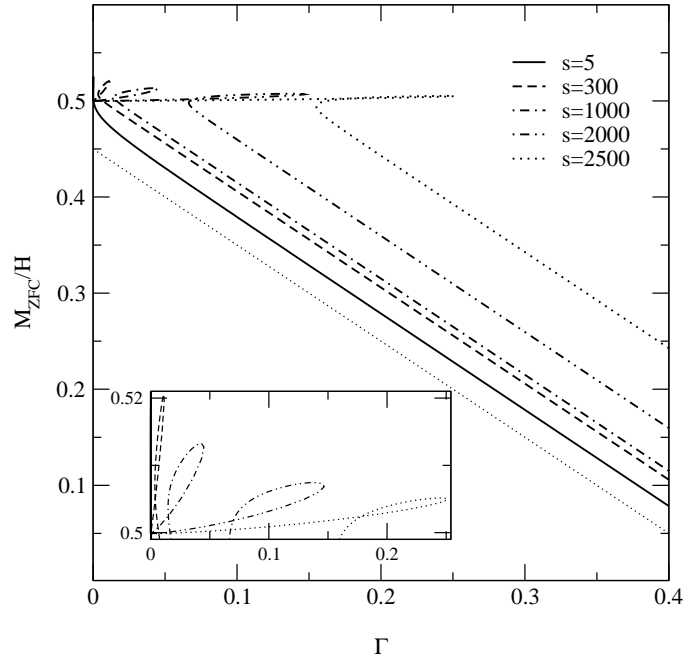


Figure 5:  $M_{\text{ZFC}}/H$  vs.  $\Gamma$ , where the parameters are as in figure 4. For reference, the grey line gives the curve  $M_{\text{ZFC}}/H = 1\Gamma$ . In the inset the region of the loops is shown in more detail.

## 6 Dynamics in an oscillating field

Further aspects of the magnetization reversal transitions become apparent when the response of the system to a time-dependent external field  $H = H(t)$  is studied. This allows to study hysteresis effects – related to the easily measured Barkhausen noise – and has been studied for a long time, see [6, 7] for reviews. From mean-field descriptions [35, 36, 57], one finds evidence that, depending on the amplitude and the period  $P$  of  $H(t)$ , the time-dependent (and periodic) magnetization  $S(t) = S(t + P)$  changes between two different forms. First, there is a single symmetric solution (corresponding to the paramagnetic phase) such that

$$S(t + P/2) = -S(t). \quad (6.1)$$

Second, there may exist a pair of non-symmetric solutions in the ferromagnetic phase where (6.1) does not hold. Indeed, the existence of a dynamical phase transition was established beyond mean-field theory through simulations in the 2D Ising model with Glauber dynamics [29, 30, 31]. The order parameter of this transition is the period-averaged magnetization  $Q = Q(t)$  defined as

$$Q(t) = \frac{1}{P} \int_{t-P}^t dt' S(t'), \quad (6.2)$$

where  $P$  is the period of  $H(t)$ . In the Ising model for sufficiently strong fields and/or low frequencies  $Q = 0$  and  $S(t)$  oscillates around zero, but  $Q$  remains finite for smaller fields and higher frequencies and  $S(t)$  then oscillates around one of the two values of the equilibrium magnetization. Detailed finite-size scaling analysis has shown that the exponents of  $Q(t)$  and also of the associated susceptibility agree with those of the *equilibrium* phase transition of the 2D Ising model [29, 30, 33].

Still, this kind of non-equilibrium phase transition need not generically exist. In the  $q$ -states Potts model with  $q \geq 3$ , for example, a mean-field analysis shows that the time-dependent order parameter undergoes a cascade of period-doubling bifurcations, rather than a simple phase transition [36]. It is

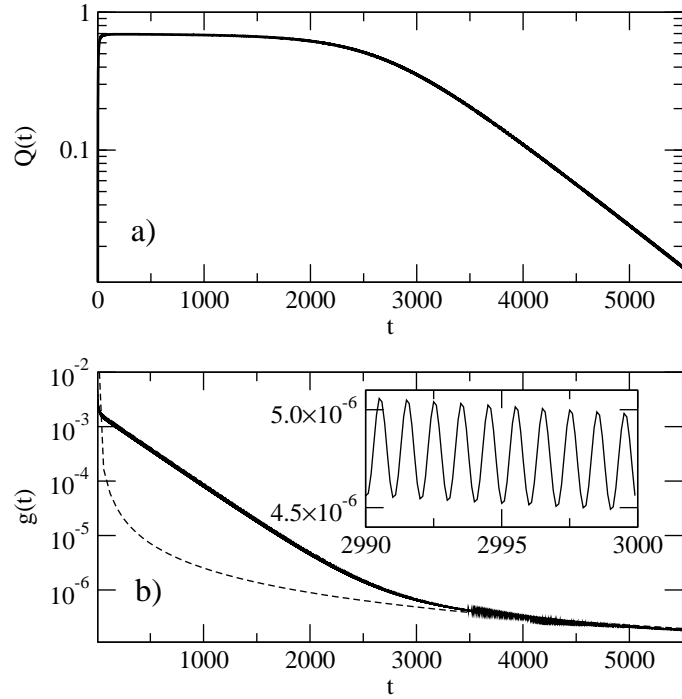


Figure 6: (a) The period-averaged magnetization  $Q(t)$  for  $d = 3$ ,  $T = 2$ ,  $S_0 = 0$ , a sinusoidal external field with period  $P = 1.5$  and amplitude  $H_0 = 0.2$ . (b) The Lagrange multiplier  $g(t)$ . On this scale only the behaviour of the bounds can be seen between which oscillations take place; these oscillations are shown in the inset. The dashed line shows a power law  $g(t) = 0.1 t^{-1.54} \approx c \cdot t^{-d/2}$ .

therefore of interest to explore the role of the topology of the phase space further by considering a model in a different equilibrium universality class.

## 6.1 Behaviour of the magnetization

We consider the spatially constant but time-dependent external field

$$H(t) = H_0 \sin\left(\frac{2\pi}{P}t\right). \quad (6.3)$$

The calculation of the observables follows the same lines as in the case of the constant field although a larger numerical effort is required. By inserting eq. (3.10) into eq. (6.2) the period-averaged magnetization  $Q(t)$  is readily obtained. In figure 6a a typical example for  $Q(t)$  is shown but the behaviour seen in this case turns out to be generic. Taking the Ising model as a guide, a heuristic argument [36] suggests that a dynamic phase-transition should occur at least for all temperatures and field amplitudes  $H_0$  for which a metastable state exists. We therefore used the same values for  $T$  as before. However, in the spherical model we find that for small times  $Q(t)$  takes a plateau value before it decays exponentially for later times. In principle, and in analogy with the Ising model, one might try to find the dynamic phase transition by measuring the time  $\tau = \tau(P, H_0)$  when the transition between the plateau and the decay occurs. Following the practical experience of the Ising model either the scale of  $H$  or  $P$  can be normalized away, see [29, 30, 31]. It should therefore be enough to vary the period  $P$  (or the frequency) but keep the amplitude  $H_0$  constant and map out  $\tau(P, H_0)$ . If there is a dynamic phase transition at some critical period  $P_c$ , the cross-over time should diverge  $\tau(P_c, H_0) = \infty$ . In practice, however, this method is quite slow, because the calculations have to be done for increasingly larger time-scales.

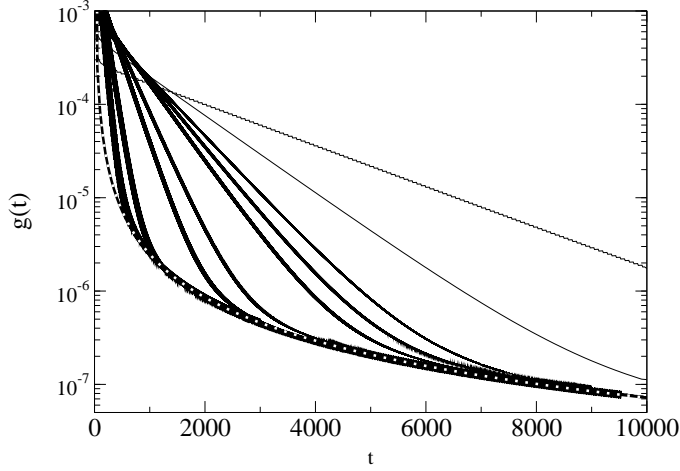


Figure 7:  $g(t)$  for  $d = 3$ ,  $T = 2$  and a sinusoidal external field with  $H_0 = 0.2$ ; the periods are  $P = \{0.4; 0.6; 0.8; 0.9; 1; 1.5; 2; 5; 10\}$  (from top to bottom). The dashed line shows a function  $g_{\text{mas}}(t) = 0.1 t^{-1.54} \approx c \cdot t^{-d/2}$

It is a lot more efficient to study the Lagrange multiplier  $g(t)$  which is shown in figure 6b. We observe that the value of  $g(t)$  oscillates between two bounds and the temporal behaviour of the bounds correlates with the time-dependence of  $Q(t)$ . Namely, when  $Q(t)$  displays a plateau, the bounds for  $g(t)$  decay exponentially with time while in the region of the exponential decay of  $Q(t)$  the bounds of  $g(t)$  decay with according to a power law. Therefore, the cross-over time  $\tau(P, H_0)$  can be found by determining the intersection of the two regimes for the bounds for  $g(t)$ .

In figure 7 we display a typical behaviour of  $g(t)$  for several values of the period  $P$ . We observe the cross-over from a roughly exponential behaviour  $g_{\text{exp}}(t) \approx \exp(-t/\tau)$  with a relaxation time  $\tau$  towards a master curve  $g_{\text{mas}}(t) \sim t^{-1.54}$  which is reached for all given values of  $P$  for sufficiently long times. In principle, one might try to estimate the time of cross-over between these two regimes by looking for the intersection of  $g_{\text{exp}}(t)$  and  $g_{\text{mas}}(t)$  and then further ask when this cross-over time will diverge in order to find the critical period  $P_c$ . Since for finite  $\tau$  this intersection will always occur, a more reliable estimate of  $P_c$  will be given by the

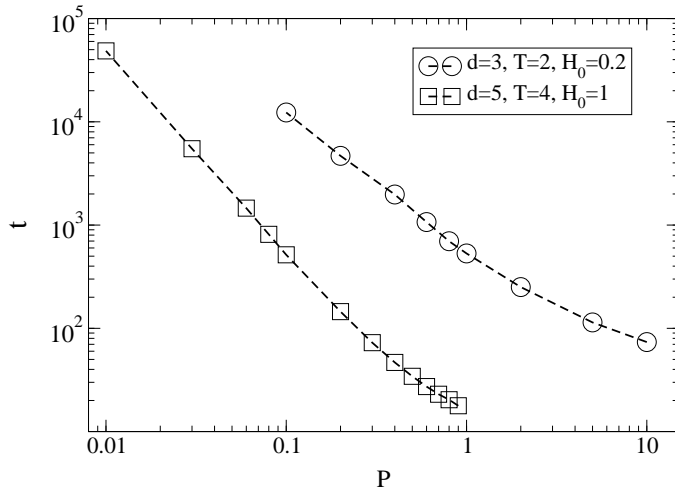


Figure 8:  $\tau(P, H_0)$  for  $d = 3$  and  $d = 5$  as read off from  $g_{\text{exp}}(t)$ , see text.

In figure 8 we show  $\tau(P, H_0)$  for  $d = 3$  and  $d = 5$ , that is below and above the upper critical

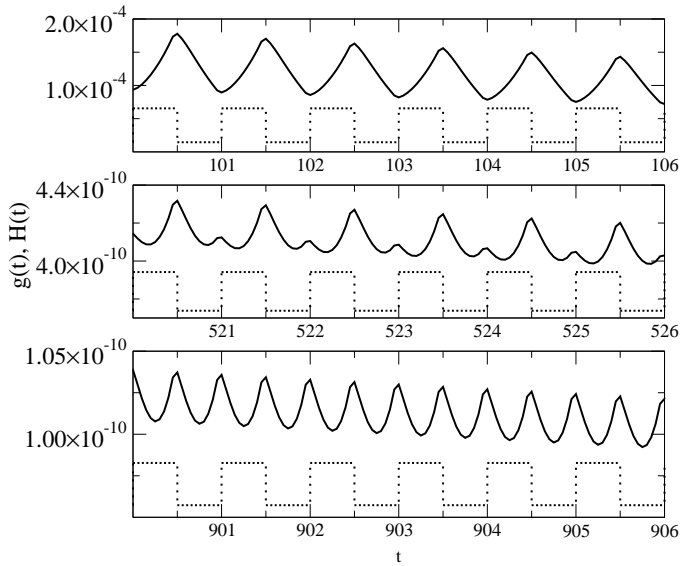


Figure 9:  $g(t)$  (full line) compared to  $H(t)$  (dotted line, scaled and shifted) for different times. These calculations were done for  $d = 5$ ,  $T = 4$ ,  $S_0 = 0$  and a rectangular external field with amplitude  $H_0 = 0.6$  and with period  $P = 1$ .

dimension of the equilibrium critical behaviour. In all curves, we see that  $\tau(P)$  remains finite for all values of  $P$  which we considered. Phenomenologically,  $\tau \sim 1/P^v$  for  $P$  small enough and some exponent  $v > 0$  ( $v \approx 1.4$  in  $3D$ ;  $v \simeq 1.95$  in  $5D$ ). The fact that  $\tau$  only diverges as  $P \rightarrow 0$  is evidence that there is *no DPT* in the spherical model in an oscillating magnetic field, in contrast to established results [29, 30, 31, 33] in the 2D Ising model. We also see from figure 8 that the absence of the DPT is not related to whether or not the equilibrium phase transition of the spherical model is in the mean-field regime.

## 6.2 Behaviour of the Lagrange multiplier

By fitting  $g_{\text{mas}}(t)$  for  $d = 3$  and  $d = 5$  we find exponents of  $w = 1.52 \pm 0.01$  and  $w = 2.51 \pm 0.01$  respectively. From these observations, we conjecture that for sufficiently long times, the Lagrange multiplier  $g(t)$  satisfies the bounds

$$C_1 \leq t^w g(t) \leq C_2 \quad (6.4)$$

with an exponent  $w = d/2$  and some constants  $C_{1,2}$ . Indeed, we have also checked that these bounds hold not only for sinusoidal fields  $H(t)$ , but for triangular and rectangular oscillating fields as well. Remarkably, the conjectured exponent  $w = d/2$  of the power-law bounds eq. (6.4) coincides with the same value found for the kinetic spherical model *without* a magnetic field [47]! We have checked this for several values of the dimension  $d$ . In appendix B, we derive the bounds (6.4) and especially the exponent  $w = d/2$  in the  $P \rightarrow 0$  limit and for  $T=0$ , under mild additional conditions. A fully disordered initial state simplifies the calculations but the result remains the same for any short-ranged initial correlators. Therefore, the relaxation time  $\tau(P, H_0)$  is formally infinite for  $P \ll 1$  and  $T = 0$ . We have thus shown the *absence of a DPT in the physical situation where it would have been expected to be seen first*. In this respect, the spherical model behaves in quite a different way than the Ising model. The rigorous derivation of eq. (6.4) is left as an open mathematical problem.

The absence of a dynamical phase transition is further illustrated in figure 9. There we compare  $g(t)$  with a rectangular field  $H(t)$  (scaled and shifted for convenience). While for small times,  $g(t)$

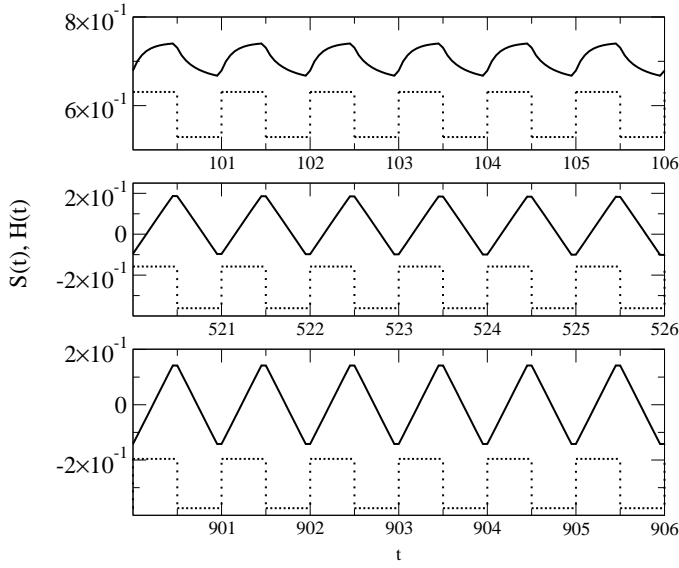


Figure 10: Time evolution of the mean magnetization  $S(t)$  (full line) compared to the one of a rectangular magnetic field  $H(t)$  (dotted line, scaled and shifted) for different time regimes; the parameters are as in fig. 9.

oscillates with the driving period  $P$ , we see that with  $t$  increasing, an additional peak builds up until  $g(t)$  oscillates with half the period of the driving field at late times. The fact that  $g(t)$  oscillates with half the external period  $P$  is an indication that the system is described by the symmetric solution, see eq. (6.1). The same kind of period-halving is also found for triangular and sinusoidal fields.

This phenomenon is easily understood: since for small times the magnetization oscillates around a non-vanishing value, the global symmetry is broken and the two half-periods of the external field affect the system in two qualitatively different ways. However, for later times the magnetization oscillates around zero and there is no qualitative difference of the response of the system between the two half-periods of the external field any more. This fact is reflected by  $g(t)$  actually becoming periodic with period  $P/2$ , viz.  $g(t + P/2) = g(t)$ .

The behaviour of  $S(t)$  is illustrated in figures 10, 11, and 12. For relatively small times (upper panel),  $S(t)$  oscillates around the positive equilibrium value and is periodic with period  $P$ . It is interesting to note that the qualitative shape of  $S(t)$  for the rectangular oscillating external field in this regime matches closely the one observed in the dynamically ordered phase of the 2D Ising model, see [30, figure 2(b)]. For larger times, the dynamic order parameter  $Q(t)$  decreases until  $S(t)$  oscillates around zero. The slow cross-over towards a solution which satisfies eq. (6.1) is illustrated in the middle panels of figures 10-12 and in the lowest panels, a situation near to (6.1) is reached, where  $S(t)$  becomes *antiperiodic* with period  $P/2$ . In the case of a rectangular field shown in figure 10 the external magnetic-field amplitude is still rather small which results in a linear increase and decrease of the magnetization. For stronger fields the magnetization reaches saturation during one half-period and the behaviour of  $S(t)$  deviates from piecewise linearity. The comparison to the sinusoidal and triangular oscillating external field shows that in all three cases the magnetization follows the integrated external field for not too large amplitudes.

The main result of this section is surprising: in spite of the fact that for  $T < T_c$  there are just two equilibrium states for both the Ising and the spherical models in a (sufficiently small) constant magnetic field, the well-established dynamic phase-transition of the Ising model in a temporally oscillating magnetic field is apparently *absent in the spherical model*.

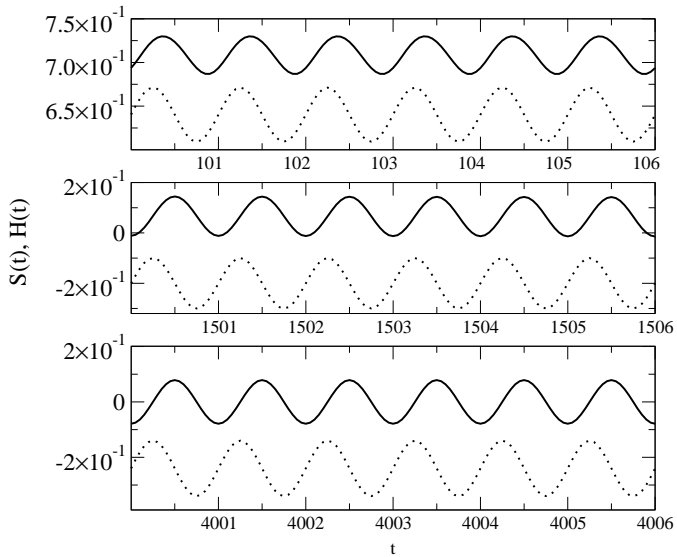


Figure 11: Time evolution of the mean magnetization  $S(t)$  (full line) compared to the one of a sinusoidal magnetic field  $H(t)$  with amplitude  $H_0 = 0.5$  (dotted line, scaled and shifted) for different time regimes; the other parameters are as in fig. 9.

## 7 Conclusions

In this paper we have investigated the non-equilibrium behaviour of the spherical model in an external magnetic field. The model's dynamics is described in terms of a Langevin equation and all quantities of physical interest can be expressed exactly in terms of the solution of a non-linear Volterra integral equation. In few especially simple cases that Volterra equation can be solved exactly, but we have in general used numerical methods.

First, we studied the magnetization reversal transition, in a temporally constant magnetic field, which occurs if the system is initially prepared in near to metastable state from which it relaxes towards to unique equilibrium state. We find that the system evolves into the metastable state quickly and remains there for considerably long times until it finally relaxes into the stable state. For not too large magnetic fields, this transition passes through transient states with long-ranged correlations of fluctuations, which means that during the magnetization-reversal transition whole domains rather than single uncorrelated spins turn over.

The two-time autocorrelation function is mainly determined by the magnetization so that connected correlation functions, which are more sensible to fluctuations, reveal more information. Again we find that the transition involves long-ranged correlations. For times smaller than the transition time  $\vartheta$  we find an effective equilibrium behaviour although the system is merely in the metastable state. In many respects, notably the fluctuation-dissipation relations, we find a close analogy with the ageing behaviour encountered in the absence of an external field. But approaching the magnetization-reversal the autoresponse function and the fluctuation-dissipation ratio show unusual behaviour, indicating that the process is rather complex. Therefore, although the non-vanishing magnetic field  $H$  sets a finite time scale for the relaxation towards the single equilibrium state, we have found a very rich transient behaviour which in many respects is quite analogous to the true ageing behaviour found without an external field.

Second, we looked for a dynamic phase transition in a time-dependent external magnetic field  $H(t)$ . Surprisingly, we find evidence that a dynamic non-equilibrium phase transition, which is known to

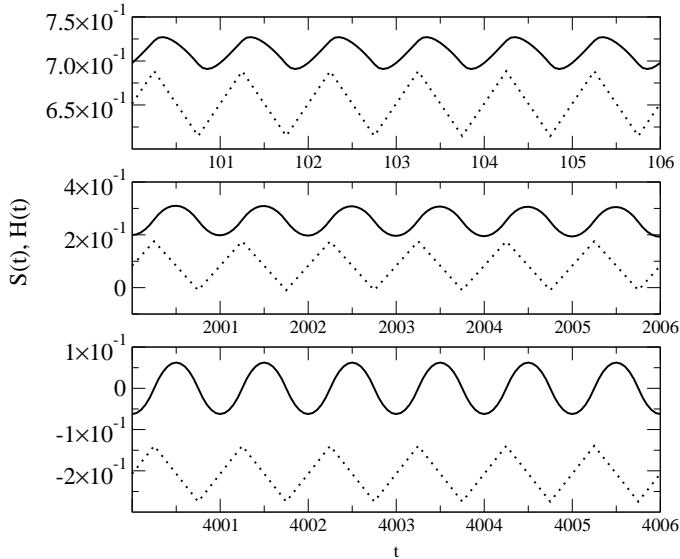


Figure 12: Time evolution of the mean magnetization  $S(t)$  (full line) compared to the one of a triangular magnetic field  $H(t)$  with amplitude  $H_0 = 0.5$  (dotted line, scaled and shifted) for different time regimes; the other parameters are as in fig. 9.

occur e.g. in the Ising model, apparently does not exist in the spherical model. For sufficiently low temperatures, we rather find that although the dynamic order parameter  $Q(t)$  reaches a plateau value for small times, there is always a cross-over to a late-time regime where  $Q(t)$  decays away to zero. On a technical level, this finding can be represented through the conjecture eq. (6.4) which points to an unexpected similarity with the phase-ordering kinetics of the *zero-field* spherical model.

Given that several equilibrium properties of the isotropic  $O(3)$  Heisenberg model are closer to the ones of the spherical model than they are to the Ising model (see introduction), our results raises the question whether a dynamic phase transition for the *isotropic*  $O(3)$  Heisenberg model in an oscillating field exists.<sup>3</sup>

Lastly, our results beg the questions what are the effects of a magnetic field on the kinetics of a spin-glass and what becomes of the magnetization reversal transition and the dynamical phase transition ? However, because of the well-known equivalence [46] between the spherical spin-glass and the spherical ferromagnet, studies in different systems with a true glassy behaviour<sup>4</sup> are needed to shed light on this issue.

<sup>3</sup>Existing articles on the DPT in Heisenberg models are either mean-field studies [34] or consider the anisotropic case [58] (which should be more Ising-like). One might anticipate the existence of a critical  $n_c$  such that in the  $O(n)$ -model in an oscillating field, there is a DPT for  $n < n_c$  analogously to the Ising model and none for  $n > n_c$ .

<sup>4</sup>The equilibrium behaviour of the Ising spin glass in a magnetic field has been studied in detail, see [59] and references therein.

## Acknowledgements

MP is grateful to the Deutscher Akademischer Austauschdienst (DAAD) for financial support (DAAD Doktorandenstipendium im Rahmen des gemeinsamen Hochschulsonderprogramms III von Bund und Ländern).

## Appendix A. Numerical method

We briefly discuss the numerical solution of the nonlinear Volterra equation (2.15), adapting standard methods [60] to the case at hand.

Eq. (2.15) is cast into the following form, using the equations (2.17) and (2.18)

$$g(t) = (1 - S_0^2) f(t) + S_0^2 + 2T \int_0^t dt' f(t - t') g(t') + 2S_0 \int_0^t dt' H(t') \sqrt{g(t')} + \left( \int_0^t dt' H(t') \sqrt{g(t')} \right)^2. \quad (\text{A1})$$

As a first step we will discretize the time by dividing the time interval in  $N - 1$  segments of length  $k$

$$t_i = k i \quad ; \quad i = 0, 1, \dots, N - 1. \quad (\text{A2})$$

The continuous functions  $f(t)$  are replaced by the  $N$  dimensional vectors

$$\mathbf{f} = (f_0, f_1, \dots, f_{N-1})^T, \quad f_i = f(t_i) \quad (\text{A3})$$

and the integrals are replaced by a sum by means of the extended trapezoidal rule [60]

$$\int_{x_0}^{x_{N-1}} dx f(x) \approx k \left[ \frac{1}{2} f_0 + f_1 + f_2 + \dots + f_{N-2} + \frac{1}{2} f_{N-1} \right]. \quad (\text{A4})$$

Therefore, we have the set of equations

$$\begin{aligned} F_0 \left( (g_0, \sqrt{g_0}), \mathbf{f}, \mathbf{H}, k \right) &= 0 \\ F_1 \left( (g_0, \sqrt{g_0}), (g_1, \sqrt{g_1}), \mathbf{f}, \mathbf{H}, k \right) &= 0 \\ &\dots \\ F_{N-1} \left( (g_0, \sqrt{g_0}), (g_1, \sqrt{g_1}), \dots, (g_{N-1}, \sqrt{g_{N-1}}), \mathbf{f}, \mathbf{H}, k \right) &= 0, \end{aligned} \quad (\text{A5})$$

depending on the known vectors  $\mathbf{f}$  and  $\mathbf{H}$  and the step size  $k$ . We have  $F_0 = g_0 - 1$  and

$$\begin{aligned} F_i \left( (g_0, \sqrt{g_0}), \dots, (g_i, \sqrt{g_i}), \mathbf{f}, \mathbf{H}, k \right) &= g_i \left[ Tk f_0 + \frac{1}{4} k^2 H_i^2 - 1 \right] \\ &+ \sqrt{g_i} \left[ S_0 k H_i + k^2 \left( \frac{1}{2} H_0 \sqrt{g_0} + \sum_{j=1}^{i-1} H_j \sqrt{g_j} \right) H_i \right] + (1 - S_0^2) f_i + S_0^2 + 2Tk \left( \frac{1}{2} f_i g_0 + \sum_{j=1}^{i-1} f_{i-j} g_j \right) \\ &+ 2S_0 k \left( \frac{1}{2} H_0 \sqrt{g_0} + \sum_{j=1}^{i-1} H_j \sqrt{g_j} \right) + k^2 \left( \frac{1}{2} H_0 \sqrt{g_0} + \sum_{j=1}^{i-1} H_j \sqrt{g_j} \right)^2 \end{aligned} \quad (\text{A6})$$

This set of equations can be solved iteratively:  $F_0$  determines  $g_0$ ,  $F_1$  then leads to  $g_1$  and so on. However, since the  $F_i$  are functions of  $g_i$  and  $\sqrt{g_i}$  at each step of iteration two *a priori* distinct solutions for the  $g_i$

are found. They may be obtained by replacing  $G_i = \sqrt{g_i}$  and solving the resulting quadratic equation in  $G_i$ . So the question arises which of these solutions has to be used.

We calculated the two solutions for  $\mathbf{g}$  when only using either the solution according to the positive root ('+'-curve) or the negative one ('-'-curve) — the exact solution should evolve somewhere between these two limiting curves. We found that decreasing the step size  $k$  results in an approach of the '-'-curve to the '+'-curve where the latter one only slightly changes. Finally choosing a sufficient small  $k$  the two curves collapse, so that the exact solution is found. For larger values of  $k$  the '+'-curve shows only small deviations to the limiting curve, so that in all calculations this solution was used.

For all calculations a step size of  $k = 10^{-2}$  was sufficient, except for the data shown in Fig. 2 where  $k = 10^{-4}$  was used because there the time scale is much smaller.

The evaluation of the one- or two-time observables proceeds by a straightforward implementation of their defining integrals by the extended trapezoidal rule.

## Appendix B.

We derive the bounds eq. (6.4) for the Lagrange multiplier  $g(t)$  in an oscillating magnetic field  $H(t)$ , for the special case of vanishing temperature  $T = 0$ . For convenience, we consider a fully disordered initial state and vanishing initial magnetization  $S_0 = 0$ , but our results also hold true for arbitrarily short-ranged initial conditions and  $S_0 \neq 0$ . We define  $G(t) := \sqrt{g(t)}$ . The non-linear Volterra integral equation then is

$$G(t)^2 = A(t) + \left( \int_0^t ds H(s) G(s) \right)^2 \quad (B1)$$

We shall assume throughout that  $G(t)$  is bounded on the positive real axis, that is  $|G(t)| \leq M < \infty$  for  $t \in [0, \infty)$ . This assumption is made plausible by our numerical results displayed in figure 9. Furthermore, we shall assume that the magnetic field itself is bounded,  $|H(t)| \leq H_0$ . It then follows from (B1) that  $|G(t)|^2 \leq A(t) + H_0^2 M^2 t^2$ . For long times, we may therefore expect a leading power-law behaviour which we may write as  $G(t) \sim t^{-w/2}$ . We wish to estimate  $w$  (the above argument gives  $w \geq -2$ ).

**Proposition:** *Let  $G(t)$  be a solution of eq. (B1) and assume that there is a constant  $M < \infty$  such that  $|G(t)| \leq M$  for all times  $t \in [0, \infty)$ . Furthermore, the oscillating field  $H(t)$  is assumed to be bounded  $|H(t)| \leq H_0$ , piecewise continuous and to have the Fourier expansion*

$$H(t) = H_0 \sum_{n=1}^{\infty} b_n \sin \left( \frac{2\pi n}{P} t \right) \quad (B2)$$

such that

$$B := \sum_{n=1}^{\infty} \frac{1}{n} |b_n| \quad (B3)$$

is convergent. Finally, let  $A(t) = f(t) = e^{-4dt} I_0(4t)^d$ , where  $I_0$  is a modified Bessel function. Then the exponent  $w$  of the asymptotic form  $G(t) \sim t^{-w/2}$  for  $t \rightarrow \infty$  is for  $P \ll 1$

$$w = \frac{d}{2} \quad (B4)$$

**Proof:** First, for *any* magnetic field  $H(t)$ , we trivially have from eq. (B1) that  $G(t)^2 \geq A(t) = f(t) = (e^{-4t} I_0(4t))^d$  and therefore, as  $t \rightarrow \infty$

$$G(t) \geq \frac{1}{(8\pi)^{d/4}} \cdot t^{-d/4} \quad (B5)$$

Consequently,  $w \leq d/2$ .

Second, we wish to find a sharp upper bound on  $G(t)$ . This requires some preparations, however. We begin by a discussion of the continuity of  $G(t)$ . Let  $\varepsilon > 0$  and consider

$$\begin{aligned} G(t + \varepsilon)^2 - G(t)^2 &= (G(t + \varepsilon) - G(t))(G(t + \varepsilon) + G(t)) \\ &= A(t + \varepsilon) - A(t) + \int_t^{t+\varepsilon} ds H(s)G(s) \left( \int_0^{t+\varepsilon} ds H(s)G(s) + \int_0^t ds H(s)G(s) \right) \end{aligned} \quad (B6)$$

Because of the first part and since  $A(t)$  decreases monotonically with  $t$ , we have  $G(t + \varepsilon) + G(t) \geq 2\sqrt{A(t + \varepsilon)}$  and obtain the estimate

$$\begin{aligned} |G(t + \varepsilon) - G(t)| &\leq \varepsilon \frac{|\dot{A}(t_A)|}{2\sqrt{A(t + \varepsilon)}} + \int_t^{t+\varepsilon} ds \frac{|H(s)G(s)|}{2\sqrt{A(t + \varepsilon)}} \left( 2 \int_0^{t+\varepsilon} ds |H(s)G(s)| + O(\varepsilon) \right) \\ &\leq \varepsilon \left[ \frac{|\dot{A}(t)|}{2\sqrt{A(t)}} + \frac{H_0^2 M^2 t}{\sqrt{A(t)}} + O(\varepsilon) \right] \end{aligned} \quad (B7)$$

Here the mean value theorem was applied to  $A(t)$  where  $t_A$  is some intermediate value,  $t_A \in [t, t + \varepsilon]$ . Taking the limit  $\varepsilon \rightarrow 0$ , we conclude that  $G(t)$  is Lipschitz-continuous. Then we can apply the mean-value theorem to eq. (B6). Because of the continuity of  $G(t)$ , the limit

$$\lim_{\varepsilon \rightarrow 0} \frac{G(t + \varepsilon) - G(t)}{\varepsilon} = \frac{\dot{A}(t)}{2G(t)} + H(t) \int_0^t ds H(s)G(s) \quad (B8)$$

exists for all times  $t \in [0, \infty)$ . Taking the derivative of (B1) with respect to  $t$ ,  $G(t)$  satisfies the differential equation

$$\dot{G}(t) = \frac{\dot{A}(t)}{2G(t)} + H(t)\sqrt{G(t)^2 - A(t)} \quad (B9)$$

Therefore, if  $H(t)$  is continuous,  $\dot{G}(t)$  is also continuous. However, if  $H(t)$  has jumps, there may be jumps in  $\dot{G}(t)$  as well.

We shall take the average of eq. (B9) over the period interval  $[t, t + P]$  of the external field. In order to prepare this, let  $\varphi(t)$  be a continuously differentiable function. Then

$$\begin{aligned} \frac{1}{P} \int_t^{t+P} ds \sin\left(\frac{2\pi n}{P}s\right) \varphi(s) &= \frac{P}{2\pi n} \cos\left(\frac{2\pi n}{P}t\right) \frac{\varphi(t) - \varphi(t + P)}{P} + \frac{1}{2\pi n} \int_t^{t+P} ds \cos\left(\frac{2\pi n}{P}s\right) \dot{\varphi}(s) \\ &= \frac{P}{2\pi n} \left[ -\cos\left(\frac{2\pi n}{P}t\right) \dot{\varphi}(t_1) + \cos\left(\frac{2\pi n}{P}t_2\right) \dot{\varphi}(t_2) \right] \end{aligned} \quad (B10)$$

where the mean-value theorems were applied and  $t_1, t_2$  are intermediate values from the interval  $[t, t + P]$ . For  $P \rightarrow 0$ , we expect  $t_1, t_2 \rightarrow \tau$ . Since  $-1 \leq \cos x \leq 1$ , we obtain the following bound for  $P \ll 1$

$$\left| \frac{1}{P} \int_t^{t+P} ds \sin\left(\frac{2\pi n}{P}s\right) \varphi(s) \right| \leq \frac{P}{\pi n} |\dot{\varphi}(\tau)| + o(P) \quad (B11)$$

Before carrying out the average over eq. (B9), we consider the approximation of  $H(t)$  as given by eq. (B2) through a finite Fourier-sum  $H_N(t) := \sum_{n=1}^N b_n \sin(\frac{2\pi n}{P}t)$ . For every finite value of  $N$ ,  $H_N(t)$  is continuous and if we use  $H_N(t)$  in eq. (B9), so is  $\dot{G}(t)$ . Furthermore, if  $H(t)$  is continuous, then  $H_N(t) \Rightarrow H(t)$  converges uniformly and the  $N \rightarrow \infty$  limit and the integral may be interchanged, viz.

$$\lim_{N \rightarrow \infty} \int dt H_N(t) \varphi(t) = \int dt H(t) \varphi(t) \quad (\text{B12})$$

where  $\varphi(t)$  is some suitable function. If on the other hand  $H(t)$  is only piecewise continuous, we only have point-wise convergence  $H_N(t) \rightarrow H(t)$ . In this case, the well-known Gibb's phenomenon occurs which states that close to jump discontinuities the trigonometric approximations  $H_N(t)$  overshoot the limit  $H(t)$  by about 9% of the jump height, see [61]. Because  $H(t)$  is bounded, we certainly have the bound  $|H_N(t)| \leq 2H_0$  for all  $N \in \mathbb{N}$  sufficiently large. Then the conditions of Lebesgue's theorem, see [61], are satisfied and one arrives again at (B12).

Averaging eq. (B9) over a period interval, we obtain

$$\frac{1}{P} \int_t^{t+P} ds \dot{G}(s) = \frac{1}{P} \int_t^{t+P} ds \frac{\dot{A}(s)}{2G(s)} + \frac{1}{P} \lim_{N \rightarrow \infty} \int_t^{t+P} ds H_N(s) \sqrt{G(s)^2 - A(s)} \quad (\text{B13})$$

We now consider  $P \ll 1$ . The left-hand side and the first term on the right-hand side are estimated by the mean-value theorem. For the second term, we use the inequality (B11) term by term, taking the  $N \rightarrow \infty$  limit at the end. This gives, up to terms of order  $\text{o}(P)$

$$\begin{aligned} |\dot{G}(\tau)| &\leq \frac{1}{2} \left| \frac{\dot{A}(\tau)}{G(\tau)} \right| + \left| \frac{d}{d\tau} \sqrt{G(\tau)^2 - A(\tau)} \right| \frac{H_0 P}{\pi} \sum_{n=1}^{\infty} \frac{|b_n|}{n} \\ &\leq \frac{1}{2} \left| \frac{\dot{A}(\tau)}{G(\tau)} \right| + \frac{H_0 P B}{\pi} \left| \frac{\dot{A}(\tau)}{2\sqrt{G(\tau)^2 - A(\tau)}} \right| + \frac{H_0 P B}{\pi} \frac{G(\tau)}{\sqrt{G(\tau)^2 - A(\tau)}} |\dot{G}(\tau)| \end{aligned} \quad (\text{B14})$$

where the condition (B3) was used. We finally arrive at

$$|\dot{G}(\tau)| \leq \left| \frac{\dot{A}(\tau)}{2G(\tau)} \right| \Phi \left( \frac{H_0 P B}{\pi}, \frac{A(\tau)}{G(\tau)^2} \right) ; \quad \text{where } \Phi(\alpha, x) := \left| \frac{1 + \frac{\alpha}{\sqrt{1-x}}}{1 - \frac{\alpha}{\sqrt{1-x}}} \right| \quad (\text{B15})$$

We now assume that the strict inequality  $w < d/2$  holds. For large values of  $t$ , we then have  $A(t)/G(t)^2 \sim t^{w-d/2} \rightarrow 0$ . On the other hand, the function  $\Phi(\alpha, x)$  has a pole at  $x_c = 1 - \alpha^2 = 1 - (H_0 P B / \pi)^2$ . There is a  $t_0$  sufficiently large, such that, say,  $A(t_0)/G(t_0)^2 \leq x_c/2$  and for  $\tau \geq t_0$ , we have  $\Phi(\alpha, A(\tau)/G(\tau)^2) \leq \Phi(\alpha, x_c/2)$ , which is finite. In addition, for uncorrelated initial conditions  $A(t) = f(t)$ , thus  $\dot{A}(t) = 4de^{-4dt} I_0(4t)^{d-1} [I_1(4dt) - I_0(4dt)] \sim t^{-d/2-1}$ . Inserting these asymptotic forms into eq. (B15), we find  $d/2 \leq w$  in contradiction with the assumption  $w < d/2$ . q.e.d.

The condition (B3) is trivially satisfied for a sinusoidal field. For a triangular field, one has  $b_n \sim n^{-2}$  and for a rectangular field,  $b_n \sim n^{-1}$ . In both cases  $B$  is a finite constant and we have  $w = d/2$ , in agreement with our numerical observation.

For any short-ranged initial condition,  $A(t) \sim t^{-d/2}$  and our result  $w = d/2$  stays the same. On the other hand, for long-range initial correlations of the form  $C_{\text{ini}}(\mathbf{r}) \sim |\mathbf{r}|^{-d-\alpha}$  with  $\alpha < 0$  [11], we obtain in the same way  $w = (d + \alpha)/2$ .

Finally, for a non-vanishing initial magnetization  $S_0 \neq 0$ , we have

$$\dot{G}(t) = \frac{\dot{A}(t)}{2G(t)} + S_0 H(t) + H(t) \sqrt{G(t)^2 - A(t)} \quad (\text{B16})$$

Since  $\int_t^{t+P} ds H(s) = 0$ , the exponent  $w = d/2$  is unchanged.

## References

- [1] L.C.E. Struik, *Physical aging in amorphous polymers and other materials*, Elsevier (Amsterdam 1978)
- [2] A.J. Bray, Adv. Phys. **43**, 357 (1994).
- [3] M.E. Cates and M.R. Evans (eds), *Soft and Fragile Matter*, IOP Press (Bristol 2000).
- [4] C. Godrèche and J.M. Luck, J. Phys. Cond. Matt. **14**, 1589 (2002).
- [5] L.F. Cugliandolo, [cond-mat/0210312](https://arxiv.org/abs/cond-mat/0210312).
- [6] J.P. Sethna, O. Perkovic and K.A. Dahmen, [cond-mat/9704059](https://arxiv.org/abs/cond-mat/9704059).
- [7] P.A. Rikvold, G. Brown, S.J. Mitchell and M.A. Novotny, [cond-mat/0110103](https://arxiv.org/abs/cond-mat/0110103).
- [8] M. Henkel, M. Paessens and M. Pleimling, Europhys. Lett. **62**, 664 (2003).
- [9] D.S. Fisher and D.A. Huse, Phys. Rev. **B38**, 373 (1988).
- [10] D.A. Huse, Phys. Rev. **B40**, 304 (1989).
- [11] A. Picone and M. Henkel, J. Phys **A35**, 5575 (2002).
- [12] C. Yeung, M. Rao and R.C. Desai, Phys. Rev. **E53**, 3073 (1996).
- [13] G. Schehr and P. Le Doussal, [cond-mat/0304486](https://arxiv.org/abs/cond-mat/0304486).
- [14] M. Henkel, M. Pleimling, C. Godrèche and J.-M. Luck, Phys. Rev. Lett. **87**, 265701 (2001).
- [15] M. Henkel, Nucl. Phys. **B641**, 405 (2002).
- [16] M. Henkel and J. Unterberger, Nucl. Phys. **B660**, 407 (2003).
- [17] M. Henkel and M. Pleimling, [cond-mat/0302482](https://arxiv.org/abs/cond-mat/0302482).
- [18] L.F. Cugliandolo and J. Kurchan, J. Phys. **A27**, 5749 (1994).
- [19] L.F. Cugliandolo, J. Kurchan, and G. Parisi, J. Physique **I4**, 1641 (1994).
- [20] A. Garriga, J. Phys. Cond. Matt. **14**, 1581 (2002)
- [21] A. Pérez-Madrid, D. Reguera and J.M. Rubí, J. Phys. Cond. Matt. **14**, 1651 (2002) and [cond-mat/0210089](https://arxiv.org/abs/cond-mat/0210089).
- [22] T.S. Grigera and N.E. Israeloff, Phys. Rev. Lett. **83**, 5038 (1999).
- [23] D. Hérisson and M. Ocio, Phys. Rev. Lett. **88**, 257202 (2002).
- [24] L. Bellon and S. Ciliberto, Physica **D168-169**, 325 (2002).
- [25] W. Wernsdorfer, K. Hasselbach, A. Benot, B. Barbara, B. Doudin, J. Meier, J.-Ph. Ansermet, D. Mailly, Phys. Rev. **B55**, 11552 (1997).

[26] S. Mangin, A. Sulpice, G. Marchal, C. Bellouard, W. Wernsdorfer and B. Barbara, Phys. Rev. **B60**, 1204 (1999).

[27] S. Ludwig and D.D. Osheroff, [cond-mat/0305120](#).

[28] K. Brendel, G.T. Barkema et H. van Beijeren, [cond-mat/0210370](#)

[29] S.W. Sides, P.A. Rikvold and M.A. Notvotny, Phys. Rev. **E59**, 2710 (1999).

[30] G. Korniss, C.J. White, P.A. Rikvold and M.A. Notvotny, Phys. Rev. **E63**, 016120 (2000)

[31] G. Korniss, P.A. Rikvold and M.A. Notvotny, Phys. Rev. **E66**, 056127 (2002).

[32] A.P. Mehta, A.C. Mills, K. Dahmen and J.P. Sethna, Phys. Rev. **E65**, 046139 (2002).

[33] A. Chatterjee and B.K. Chakrabarti, Phys. Rev. **E67**, 046113 (2003).

[34] V. Turkowski, V.R. Vieira and P.D. Sacramento, [cond-mat/0305139](#).

[35] T. Tomé and M.J. de Oliveira, Phys. Rev. **A41**, 4251 (1990).

[36] J.F.F. Mendes and E.J.S. Lage, J. Stat. Phys. **64**, 653 (1991).

[37] A.J. Bray, K. Humayun and T.J. Newman, Phys. Rev. **B43**, 3699 (1991).

[38] H.K. Janssen, B. Schaub and B. Schmittmann, Z. Phys. **B73**, 539 (1989).

[39] T.J. Newman and A.J. Bray, J. Phys. **A23**, 4491 (1990).

[40] J.G. Kissner and A.J. Bray, J. Phys. **A26**, 1571 (1993).

[41] A. Coniglio, P. Ruggiero and M. Zanetti, Phys. Rev. **E50**, 1046 (1994).

[42] P. Calabrese and A. Gambassi, Phys. Rev. **E65**, 066120 (2002); **B66**, 212407 (2002); **E66**, 066101 (2002); **E67**, 036111 (2003).

[43] N. Fusco and M. Zannetti, Phys. Rev. **E66**, 066113 (2003).

[44] L.F. Cugliandolo and D.S. Dean, J. Phys. **A28**, 4213 (1995).

[45] L.F. Cugliandolo and D.S. Dean, J. Phys. **A28**, L453 (1995).

[46] W. Zippold, R. Kühn and H. Horner, Eur. Phys. J. **B13**, 531 (2000).

[47] C. Godrèche and J.M. Luck, J. Phys. **A33**, 9141 (2000).

[48] S.A. Cannas, D.A. Stariolo and F.A. Tamarit, Physica **A294**, 362 (2001).

[49] F. Corberi, E. Lippiello and M. Zanetti, Phys. Rev. **E65**, 046136 (2002).

[50] A. Picone, M. Henkel and J. Richert, J. Phys. **A36**, 1249 (2003).

[51] M.A. Abramowitz and I.A. Stegun, *Handbook of Mathematical Functions*, Dover (New York 1965)

[52] N.K. Karapetyants, A.A. Kilbas, M. Saiko and S.G. Samko, J. Integral Equations Appl. **12**, 421 (2000).

- [53] L. Berthier, P.C.W. Holdsworth, and M. Sellitto, J. Phys. **A34**, 1805 (2001).
- [54] C. Chatelain, [cond-mat/0303545](https://arxiv.org/abs/cond-mat/0303545).
- [55] G. Baéz, H. Larralde, F. Levyraz and R.A. Méndez-Sánchez, Phys. Rev. Lett. **90**, 135701 (2003).
- [56] G. Parisi, F. Ricci-Tersenghi, and J.J. Ruiz-Lorenzo, Eur. Phys. J. **B11**, 317 (1999).
- [57] H. Fujisaka, H. Tutu and P.A. Rikvold, Phys. Rev. **E63**, 036109 (2001).
- [58] H. Jang and M.J. Grimson, Phys. Rev. **E63**, 066119 (2001); H. Jang, M.J. Grimson and C.K. Hall, Phys. Rev. **B67**, 094411 (2003).
- [59] I.R. Pimentel, T. Temesvári and C. DeDominicis, Phys. Rev. **B65**, 224420 (2002).
- [60] W.H. Press, S.A. Teukolsky, W.T. Vetterling and B.P. Flannery, *Numerical Recipes*, 2<sup>nd</sup> edition, Cambridge University Press (1992); section 18.2.
- [61] R. Courant and D. Hilbert, *Methoden der Mathematischen Physik I*, 3<sup>rd</sup> edition, Springer (Heidelberg 1968), pp 90-93.